

# Wireless soil moisture sensor networks for agriculture

Sanjaya Gurung  
Electrical Engineering Dept.  
University of North Texas  
Denton, Texas  
sanjayagurung@my.unt.edu

Siddharth Thakur  
Electrical Engineering Dept.  
University of North Texas  
Denton, Texas  
SiddharthThakur@my.unt.edu

Breana Smithers  
Electrical Engineering Dept.  
University of North Texas  
Denton, Texas  
Breana.Smithers@unt.edu

Miguel Acevedo  
Electrical Engineering Dept.  
University of North Texas  
Denton, Texas  
acevedo@unt.edu

**Abstract** —Over 60% of agricultural water is wasted due to inefficient irrigation that results from a lack of crop and soil monitoring. Most solutions to this problem are either too expensive for small farmers or lack feasibility of implementation in large-scale commercial farms. A soil moisture wireless sensor network is a promising solution, which can be readily deployed in small, as well as commercial farms, and has been proven to increase irrigation efficiency. However, these systems are generally expensive or are not thoroughly designed for all situations. We propose and test a Wireless Soil Moisture Sensor Network for Agriculture as a system of interconnected, self-sufficient, solar-powered sensor nodes and centralized gateways. Thus, providing farmers with real-time information of soil-moisture, soil-temperature, relative humidity, and weather. Six nodes and one gateway were deployed and tested for four months, and have proven to be reliable and self-sufficient, all while continuing to transmit sensor data, which is successfully logged by the centralized gateway onto a website capable of time-based graphical analysis. The system has also shown to be easily adaptable, as changes and modifications were made to the network. In addition, the proposed system is comprehensive, cost-effective, and scalable. It can be deployed in both commercial and small farms so that farmers can make informed decisions on irrigation and crop management, which consequently increases irrigation efficiency and agricultural productivity.

**Keywords**—soil moisture, wireless sensor networks, agriculture, irrigation, irrigation efficiency, low power.

## I. INTRODUCTION

Agriculture accounts for over 60% of the world's water consumption, however with typical farming irrigation efficiencies of 40%, over 60% of agricultural water is wasted, contributing to rising poverty and famine levels impacting over 2.5 billion people [1]. In the US, agriculture, with economic output of 152 billion dollars [2] accounts for ~80% of water consumption, with irrigated agriculture accounting for ~40% of agricultural sales. However, in recent years, the amount of irrigated land has reduced, as severe droughts and water-scarcity affected regions in the Western US; a region representing 78.8% of all irrigated production. Therefore, it is necessary to develop a solution to increase irrigation efficiency, which is defined as the percentage of applied irrigation water that is beneficially used and not lost [2]. Specifically, around 10-15% of all agricultural irrigation water is lost due to overwatering of crops.

Solutions to irrigation water loss include adopting newer technology, installing infrastructure such as recycling systems,

Partial funding support was provided by the Innovations at the Nexus of Food, Energy, and Water Systems (INFEWS) program of the National Science Foundation under award number 1856052.

reconfiguring irrigation layouts, and developing infrastructure to improve in-field application systems. Opportunities to improve food production via increased water productivity (i.e., more food per unit of water) include technology, e.g., monitoring field conditions, amenable to be adopted by farmers [3]. Monitoring soil moisture is one of the most promising technical solutions to reduce overwatering, as it is a simple and effective way to provide information for a farmer to regulate the irrigation of their crops. Furthermore, all other solutions either require a major overhaul of preexisting systems or the cost is relatively higher in comparison to the installation of a soil-moisture sensing network. In addition, to determine crop water requirements, climate conditions such as intensity of sunlight, temperature, and humidity must be monitored due to their effect on evapotranspiration rates [2].

Measuring water content in the soil by electronic devices is based on soil electrical properties, such as dielectric constant (i.e. relative permittivity), and soil conductivity. Relative permittivity has shown to be an effective estimator of soil moisture, and several techniques are used to relate the response of an electric circuit to relative permittivity [4, 5]. Among these techniques, time domain reflectometry (TDR)[5-7] and capacitance probes [4, 5, 8, 9] are prevalent soil relative permittivity sensors. Capacitance probes are less expensive than TDR probes, therefore have become popular for developing low-cost soil moisture sensor systems [8-10]. Typically, the output of an off-the-shelf capacitance probe requires only a low direct current (DC) excitation voltage (e.g., 2-5 V), producing a signal in the order of mV, which can be converted to a digital value and calibrated to soil moisture, as volumetric water content (VWC) for various soil types. Out of several off-the-shelf capacitance probes, the Decagon's EC-5 probe is widely used [11], while Campbell Scientific TDR devices are commonly installed in weather and soil monitoring stations [12], and also integrated as portable handheld units such as the HS-2 Hydrosense II [13]. We focus on monitoring using capacitance probes, specifically an EC-5, and program calibration equations by experiments collecting voltage output concurrently with soil moisture readings from a TDR device, specifically a HS2- Hydrosense.

Two major types of temperature probes are those based on Negative Temperature Coefficient (NTC) thermistors and thermocouples. Both types of probes are used to measure temperature of air, water, and soil. Thermistors are active sensors, requiring power and a voltage divider or a bridge circuit. The output of this circuit is converted to temperature using the Steinhart-Hart model or the B equation [14]. Thermocouples produce a voltage by joining two different metals, therefore are passive sensors but require inverse polynomials to convert

voltage to temperature [14]. The metals or alloys that are joined together determine thermocouple type, e.g., copper-constantan, a Type T thermocouple. Considering low cost and ease of implementation, we focused on monitoring using thermistors and calibrated using a thermocouple-based device.

In recent years, Wireless Sensor Network (WSN) technology has been one of the top emerging applications of distributed sensing, and has been evolving into the Internet of Things. A WSN consists of sensor nodes (i.e. motes) spatially separated and wirelessly connected with each other, in a variety of topologies, and commonly connected to a gateway node. The distance between sensor nodes, ranging from tens to hundreds of meters, depends on antenna gain, transmit power, and operating frequency. WSNs environmental monitoring applications include weather and soil variables, and can combine with weather stations with wired sensors, making it easier and less expensive to expand coverage in remote areas.

One of the major challenges that WSNs have been facing is the difficulty of supplying continuous and reliable electrical power. A common practice is to use batteries; however, this requires repetitive replacement depending on various factors such as battery capacity, communication protocol, duty cycle, and average power consumption of the mote, including all connected sensors. Batteries recharged by solar PV panels can provide continuous power supply to the motes in non-shaded areas. While this technique reduces the frequency of battery replacement, it is still desirable to provide an alternate long-term solution because of numerous limitations of the battery, such as longer charging duration, shorter life cycle, and narrow operating temperature range. In addition, it is also desirable to find a more efficient solution for conditions of scarce solar resource availability, for example, the understory of tall vegetation and forests. A solution to this problem is to use

supercapacitors to store energy from the solar panels, eliminating the need to replace batteries, providing continuous power in a shaded environment.

## II. PROPOSED SYSTEM

### A. Overview

The WSN for agriculture (WSNA) is made up of a system of interconnected solar-powered sensor nodes and centralized gateways that increase irrigation efficiency by providing farmers with valuable knowledge of their farmland's soil-moisture levels, crop health, and weather, through real-time data-monitoring (Fig. 1). Specifically, a typical node in the system is an electrical device that is placed in agricultural fields to collect data from various sensors to monitor soil moisture, soil temperature, relative humidity, air temperature, and solar radiation. Each node is designed to measure soil moisture from up to three probes inserted at depths of 10, 20, and 30 cm. Each node is also self-sufficient, due to its solar energy harvester, which allows it to work off-grid without replacing batteries. Furthermore, the system can last for several days without sunlight, and if this rare event occurs, the node's backup battery can power the node for approximately four months. The node's electrical systems are enclosed in a weatherproof box, which is connected to a sturdy one-half inch diameter metal pole that is inserted at a depth of one foot in the ground. The node set up has a footprint less than six inches, allowing it to be safely placed in between crop rows so that there is no need for removal during harvesting. Thus, the system has the potential to be deployed permanently.

The implemented prototype uses Moteino (LowPowerLab) devices for nodes and gateway. Each node in a deployed WSNA is periodically queried by a gateway according to a schedule; once queried, the node packetizes the data from the sensors, as

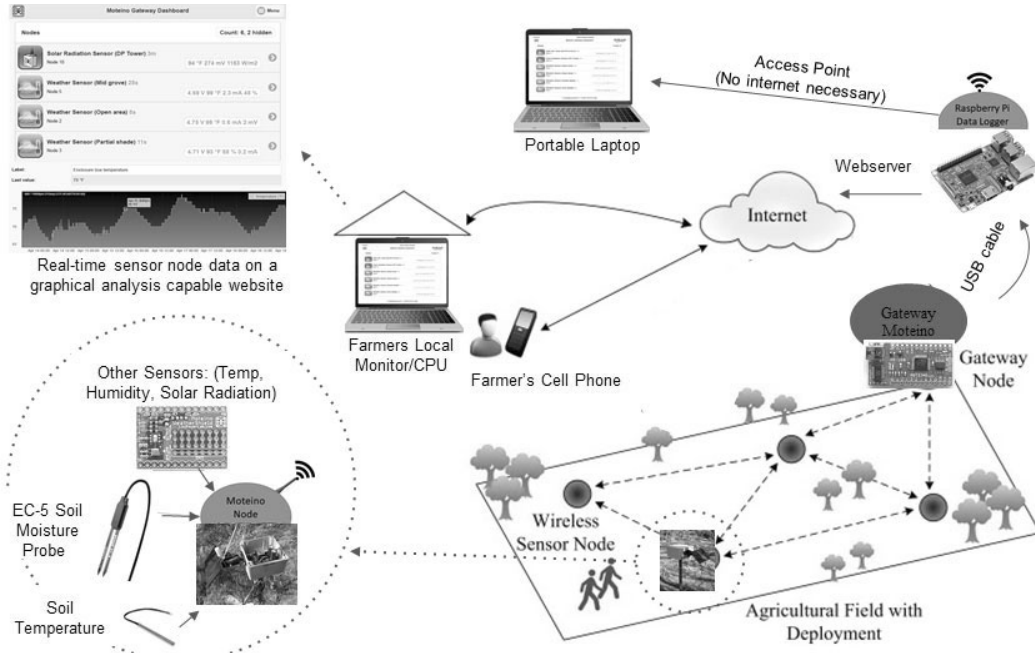


Fig. 1. Overview of a typical wireless sensor network for agriculture

well as various electrical levels in the node, and then wirelessly transmits the packet of information to the gateway over a radio signal (e.g., 915 MHz). In a typical application, each gateway controls multiple nodes, around 10-15, where each node in the gateway's cluster is placed within 300 - 400 meters away from the gateway. The gateway is a 12V DC device, and can be placed indoors or outdoors. Incoming data from the gateway is transferred to a low-cost single-board computer (e.g., Raspberry Pi), which logs the data with a timestamp and location onto a micro-SD card. A webserver in the single-board computer hosts a website, which displays the real-time data showing each node's graphical analysis in a user-friendly dashboard. The password-protected website is accessible through a web browser on any device connected to the farmer's home Wi-Fi. The webpage can also alert the farmer through text or email if critical thresholds are crossed or if the system fails. If the farm does not possess an internet connection, the system also includes the capability to broadcast its own Wi-Fi network through an access point, so that the farmer will be able to connect to the website. Another option for the farmer is to display the webpage on a dedicated monitor that is hardwired directly to the single-board computer.

It is expected that at least one node will be deployed per acre (0.404 ha) of farmland, and a maximum of 15 nodes per each gateway. This number varies, as some sources require one node per 160 acres, and some require two per 10 acres [15]. The WSNA settles on one node per acre as a good balance, though this can change based on the needs of the farm. This whole setup as previously described is adequate for small farmlands (~231 acres), which make up over 88% of all farms in the USA [16]. For larger commercial farms (>4000 acres), special equipment or software must be added to connect the system together. If the farm requires nodes to be placed farther away than 300 - 400 meters, special software can be loaded to the nodes that allow them to work as a wireless mesh network, where data "hops" from one node to the next until it reaches a gateway. Another option is to connect multiple gateways, which would add extra cost, but will allow large farms to implement the system.

### B. Node operating principle

Fig. 2 shows a detailed block diagram of the soil moisture WSN node. As the sunlight strikes the surface of the solar panel, it converts the solar energy into electrical energy. Then the current flows via the voltage regulator and the current sensor to the supercapacitors, which then start to charge. The panel keeps on charging the supercapacitors until they get fully charged, or the solar radiation goes below a threshold value. The auto balancing block controls the leakage current, hence ensures that the supercapacitors do not get overcharged. The two supercapacitors are connected in series to have a 4.8 V output.

During the charging cycle, as soon as the total voltage of the supercapacitors is equal to or greater than a certain threshold value (this value could be equal to or greater than required minimum voltage of the node), the Moteino turns on and begins data collection, transmission, and other functions. The Moteino gets its power supply, either from supercapacitors or from battery backup. The automatic switching block controls the power source providing power to the Moteino. The Moteino is powered up by supercapacitors, the primary power source, as

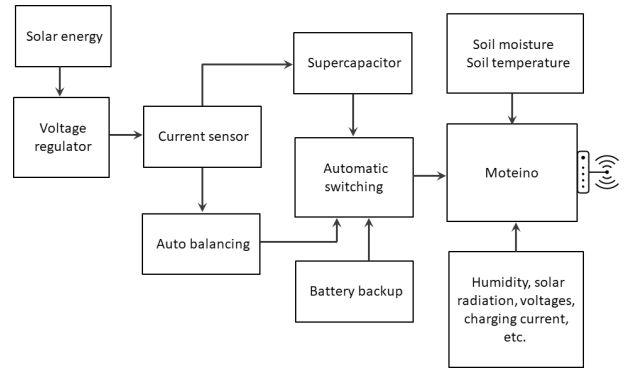


Fig. 2. WSNA node components and functional relationships

long as their combined voltage ( $V_C$ ) is greater than a certain value (3.6 V). When the combined voltage falls below this value, the power source will be automatically switched to battery backup, which is the secondary power source or alternative power source. This system allows the node to be virtually self-sufficient.

Multiple variables are measured by the sensor node including solar panel voltage, charging current, individual and total supercapacitor voltage, soil moisture, soil temperature, solar radiation, battery backup voltage, enclosure box temperature, and relative humidity. In addition, the sensor node also reports received signal strength, i.e. received signal level, and total bytes transmitted, i.e. packet length.

### C. Measuring Soil Moisture

The EC-5 soil moisture sensor was tested as a soil moisture probe for the WSNA (Fig. 3). It can be powered or excited by a supply voltage of 2.5 to 3.6V and consumes 10 mA of current [11]. The analog output voltage of the sensor can be converted into VWC by calibration. For example, using a simple linear function

$$\theta = aV_{out} + b \quad (1)$$

where  $\theta$  (in  $\text{m}^3/\text{m}^3$ ) is VWC,  $V_{out}$  is the output voltage (mV) of the sensor probe excited at 2500 mV, and coefficients  $a$  and  $b$  are determined by regression. The probe must be powered for at least 10 ms to perform a successful measurement [11]. Fig. 3 is a circuit diagram that shows how the soil moisture probe is controlled by the micro-controller through a transistor, which turns the soil moisture sensor off to help reduce power consumption when not active. When the node is queried by the

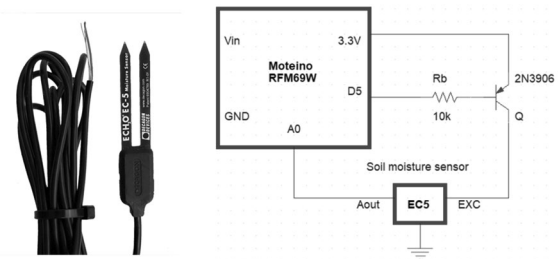


Fig. 3. Soil moisture probe and circuit to drive and read voltage output

gateway, the micro-controller activates the transistor and measures the voltage across the sensor.

The measured power consumption of this soil moisture probe is 4.3 mA in active and <1 nA in sleep state. As mentioned earlier, it is crucial to power the probe for at least 10 ms so that accurate data can be measured; we opted to set the time at 100 ms.

#### D. Measuring Soil Temperature

Two temperature sensors are used: one to measure soil temperature (built based on a NTC thermistor), and another to measure the temperature inside the enclosure box (a commercial BME280 sensor). The temperature transducer circuit using the thermistor is shown in Fig. 4. Using the voltage divider formula, the thermistor resistance is given by

$$R_{th} = (V_{cc}/V_f - 1) \times R_f \quad (2)$$

where  $R_f$  is the fixed resistor,  $R_{th}$  is the thermistor resistance that changes according to temperature, and  $V_{cc}$  is the voltage supplied to the thermistor circuit by a digital pin of the Moteino. The temperature conversion equation given by the Beta equation is,

$$T = \frac{T_0 \times \beta}{\beta + T_0 \ln(R_{th}/R_0)} \quad (3)$$

where  $T$  is in K,  $R_0$  is the value of thermistor resistance at room temperature, and  $\beta$  is a constant parameter whose value for the thermistor used (NTCLE100E3) is 3977 [17]. Temperature,  $T$ , can be further converted into Celsius or Fahrenheit according to preference. The measured power consumption of this temperature sensor is 71  $\mu$ A in active and <1 nA in sleep state. Note that for the accuracy of the sensor data, it is crucial to allow enough measurement time. The measurement time for this sensor is set as 100 ms.

#### E. Measuring solar radiation

A simple low cost pyranometer was built to record solar radiation based on a PDB-C139 photodiode that responds to light in the spectral range of 400 to 1100 nm [18]. This sensor provides its own signal without additional power consumption, except in the absence of light; however, the dark current value of the PDB-C139 photodiode is just 5 nA. The photodiode is covered with a light diffuser to achieve cosine corrected incident radiation.

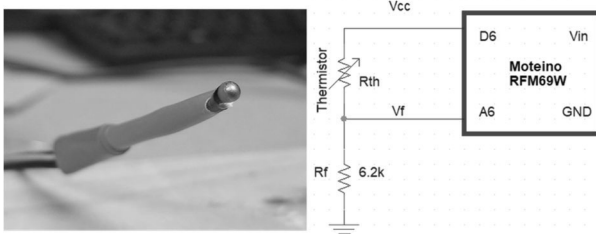


Fig. 4. Thermistor to measure soil temperature and voltage divider circuit

#### F. Gateway, Wireless Transmission, and Webpage

The centralized gateway passively queries each Moteino node in a WSNA system based on a scheduled transmission system. The node then measures all sensor data, transmits its packet to the gateway, and then goes back to sleep. The gateway processes the packet of information and sends it to the USB-connected Raspberry Pi, which logs the data onto a micro-SD card. The Raspberry Pi also runs a webserver that hosts a website, known as the Moteino Gateway Dashboard (LowPowerLab), which holds and displays all of the data from nodes in the system. Furthermore, the user-friendly dashboard displays all sensor data from each node, i.e. soil moisture, as well as a timestamp of when each value was last updated (Fig. 5). The dashboard also allows the farmer to download all data from each node in text format. Furthermore, the website shows a graphical real-time display (Fig. 6) of sensor values over time, which allows farmers to view growth and crop health over periodic seasons. This website can be accessed through any internet-connected device, allowing for portable monitoring; in non-internet situations, hardwiring and local hosting is also possible.

#### G. Power budget analysis

To develop power budget calculations we determined the average current consumption of a WSNA node at several voltage levels with the sensors connected (soil moisture probe, soil temperature sensor, solar radiation sensor, and weather shield). Two digital multimeters, Klein Tools MM600 and Agilent 34401A, were used as ammeters to measure the currents flowing into various branches of the system. The Moteino is in active mode when it wakes up from sleep mode at its scheduled transmission time, collects data from the sensors, and transmits them to the gateway before it goes back to sleep mode. For these calculations, we use an interval,  $T_p$ , of 5-minutes. A TDS 2024B Digital Oscilloscope and a 3Ω resistive dummy load were used to find the duration of the active period. From the test results, the duration of the active mode is  $T_a \approx 195$  ms, therefore the sleep mode duration is  $T_s = T_p - T_a = 299.805$  s. Current consumption

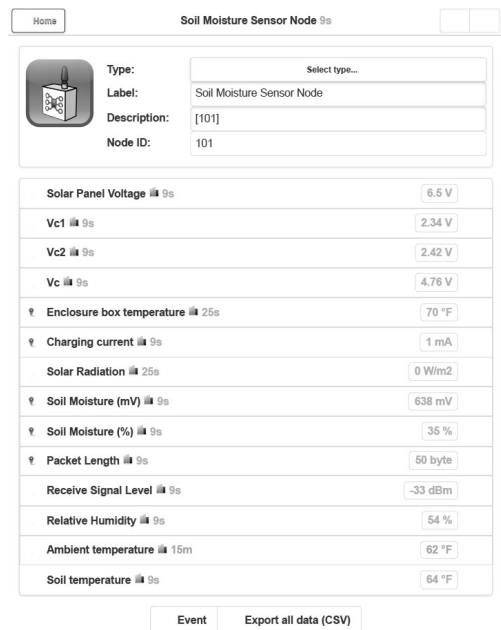


Fig. 5. Moteino gateway dashboard: illustrating typical node status and data

recorded for the active mode period is 15 mA, whereas the consumption for the sleep mode period is a function of the supercapacitor combined voltage as summarized in TABLE 1. We will focus on the highest consumption, which occurs at 4.8 V.

The total average current consumption can be calculated as

$$I_{avg} = \frac{I_s \times T_s + I_a \times T_a}{T_s + T_a} \quad (4)$$

where  $I_s$  is the current drain during the sleep period and  $I_a$  is the current drain during the active period. Substituting the values of all variables for 4.8V from TABLE 1 in equation (4), we obtain that the highest average current consumption of the WSNA node is 69.4  $\mu$ A.

With the values of average current consumption and supercapacitor size and voltage levels, the time  $T_C$  that the supercapacitors can power the system in the absence of solar energy can be calculated as

$$T_C = C_T \frac{dV_C}{I_{avg}} \quad (5)$$

where  $C_T$  is total capacitance,  $dV_C$  is voltage difference between operating voltage and threshold voltage (3.6V) to switch power to and from the backup battery. Using  $C_T = 25F$ ,  $dV_C = 4.8 - 3.6 = 1.2V$  and  $I_{avg} = 69.4\mu A$  we obtain  $T_C = 120.8h \approx 5d$ . We can say that two fully charged 3V 50F supercapacitors connected in series could power up the system with a 69.4  $\mu$ A of average power consumption for about 5 days.

Dividing battery capacity,  $C_{bat}$  by the average current consumption gives the time  $T_{bat}$  that the battery can last as

$$T_{bat} = \frac{C_{bat}}{I_{avg}} \quad (6)$$

TABLE I AVERAGE CURRENT CONSUMPTION IN SLEEP MODE OF A WSNA NODE

Component	Voltage (V)			
	4.8	4.5	3.8	3.6
Current ( $\mu$ A)				
Balancing	2.3	2.2	1.9	1.8
Moteino	52.8	52.1	49	48.1
Current sensor	2.5	2.2	1.9	1.8
Regulator	2.1	1.9	1.8	1.7
Total Current	59.7	58.4	54.6	53.4
Total Power ( $\mu$ W)	286.6	262.8	207.5	192.2

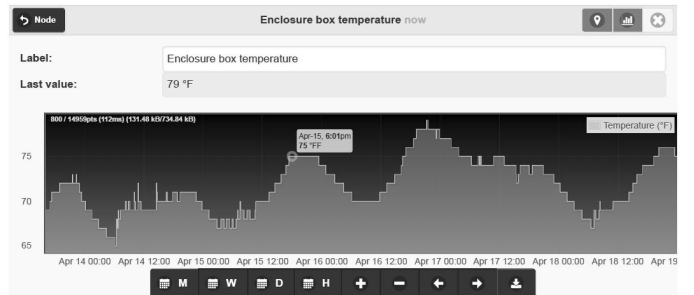


Fig. 6. Moteino gateway dashboard graphical display: example of temperature time series

substituting the values of  $C_{bat} = 200 \text{ mAh}$  and  $I_{avg} = 69.4 \mu\text{A}$ , we obtain  $T_{bat} = 2881.8 \text{ h} \approx 4 \text{ mo}$ . That is to say that a brand new 200mAh coin cell battery can power up the system with a 69.4  $\mu$ A of average power consumption for approximately 4 months.

The current consumption of an EC-5 soil moisture sensor is 4.3 mA (active) and  $<1$  nA (sleep). Similarly, the soil temperature sensor consumes 71  $\mu$ A (active) and  $<1$  nA (sleep). Combined, this pair of sensors (soil moisture probe and soil temperature sensor) consumes 4.371 mA (active) and 2 nA (sleep). The average current consumption of this pair of sensors can be calculated from equation (4) to be  $I_{avg} \approx 2.8 \mu\text{A}$ . For  $N$  additional pairs of sensors, the average current consumption will be  $I_{avg} = 69.4 \mu\text{A} + N \times 2.8 \mu\text{A}$ . For example, the average current consumption of the WSNA node with an additional two pairs of sensors will be,  $I_{avg} = 75.1 \mu\text{A}$ . To see if the node's power system can meet this increased current demand, a plot of  $T_C$  versus  $I_{avg}$  as shown in Fig. 7, was produced by simulation. We notice that, two 3V 50F supercapacitors connected in series can power the system for about 4.62 days, which means a reduction of only  $\sim 9$  h. Substituting this increased current demand  $I_{avg} = 75.1 \mu\text{A}$  in equation (6), we calculate that the

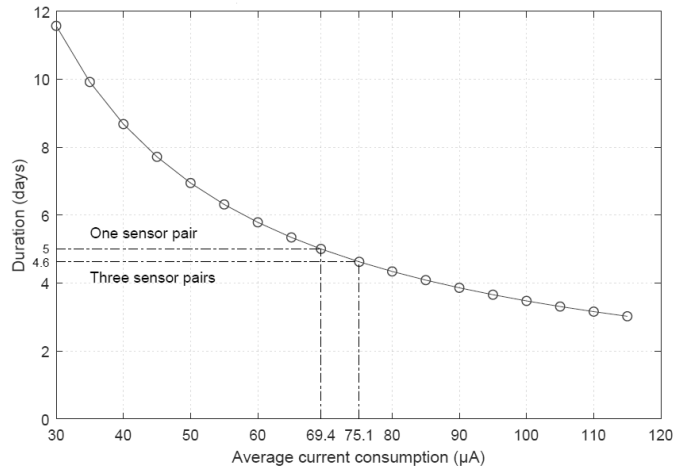


Fig. 7. Duration of super capacitor power in the absence of solar power harvesting

battery backup can last for  $T_{bat} \approx 3.65$  mo. We can say that a brand new 200mAh coin cell battery can power up the system with  $75.1 \mu\text{A}$  of average power consumption for approximately 3 months and 20 days. This means a small reduction of 10 days compared to the implemented system.

### III. BENCH-SCALE TESTS AND CALIBRATION

The EC-5 sensor was inserted into the soil at a depth of 30 cm. After adding water, it was left unattended for 5 days, then water addition was repeated, and soil moisture was recorded for one week. Soil moisture decreased gradually to 23%, and then recovered to 36% after a second addition of water. Then soil moisture slowly decreased to 28% over the period of  $\sim 5$  days, and increased rapidly again after some water was added. Subsequently, it stayed almost flat for 2 days, and after the addition of more water, the VWC rapidly increased, at which point, the value remained relatively constant.

Because the EC-5 has been validated using the gravimetric method [19] and other standard tests, we simply compared the EC-5 against a well-known TDR instrument, Hydrosense II, to obtain a calibration equation. Both sensors were inserted in the same soil at the same depth. The output voltage from the EC-5 and soil moisture data from the Hydrosense II were collected simultaneously as 30 ml/min of water was added. Linear regression (Fig. 8) yields the coefficients  $a = 0.0924$  and  $b = -32.58$ , of equation (1) which can then be programmed into the node to read VWC. We have performed this calibration with other soil samples at different ranges of VWC, including dry and wet conditions, and determined calibration equations that yield accuracy with a relative error of 1%.

Our next steps will be to calibrate the soil moisture sensor at various agricultural sites with different soil texture and composition. This will ensure that the WSNA will work in a broad variety of farmland conditions.

The photodiode yields a few millivolts when exposed to sunlight. To convert this signal into units of solar radiation, the node pyranometer was placed at the side of a commercial pyranometer, which was used as a reference. Output voltage and solar radiation data were collected simultaneously to obtain a calibration equation

$$S = cV_{out} \quad (7),$$

where  $S$  (in  $\text{W/m}^2$ ) is insolation, and  $V_{out}$  is the output voltage (mV) of the sensor, and coefficient  $c$  is 4.246.

### IV. FIELD TESTS

A WSNA pilot of six nodes and one gateway was deployed at the University of North Texas's Discovery Park in a designated outdoor research site for approximately four months. The nodes were deployed to cover a variety of conditions of insolation availability (Fig. 9).

Soil moisture data is shown in Fig. 10. The plot shows that the soil moisture value measured by the EC-5 sensor ranges from 26% to 57% of the period in the selected deployment area. While the data may not be accurate, since we did not emphasize EC-5

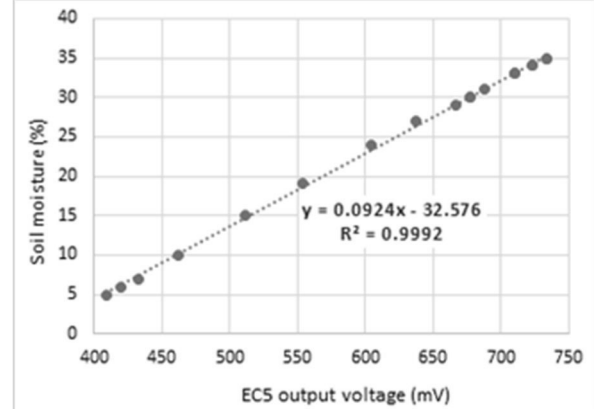


Fig. 8. Calibration of the soil moisture probe to calculate VWC from output voltage

calibration for various soil types, it shows that the soil moisture sensor EC-5 has been continuously producing the voltage signal, which is converted into VWC using the calibration equation (1).

We conducted field tests to verify the power switching function, with the first test consisting of disconnecting the solar panel from the system when the supercapacitors voltage was at its peak, allowing them to power the system without a charging source. After a few days, the voltage of the supercapacitors was below the threshold value, which is when the battery backup takes over the responsibility of powering the system. Then, the solar panel was reconnected to resume operation in harvesting mode.

From the test, we found out that the supercapacitors took five days to discharge from the initial voltage value to the threshold voltage (at which switching of power source takes place). When this value reaches 3.6 V, the supercapacitors no longer power the system, and hence, their discharging rate becomes very slow. On the other hand, the battery backup voltage was decreasing very slowly until the switching takes place, which then started discharging at a slightly faster rate. It can be easily noted that when the solar panel was reconnected after a few days, the voltage of the supercapacitors rose quickly, and the switching took place once again. This time, the load switched from battery backup to supercapacitors. As soon as this happened, the discharging rate of the battery became much slower.



Fig. 9. Deployment of a WSNA node for long-term testing under restricted sunlight conditions

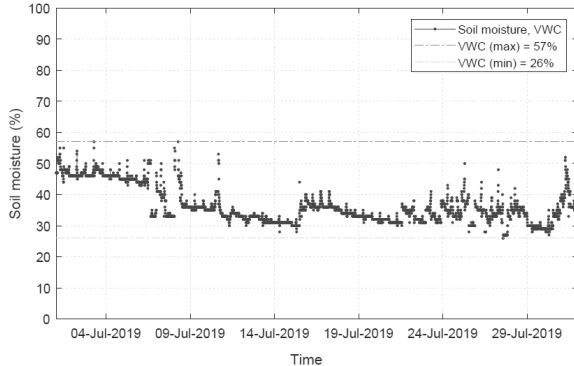


Fig. 10. Soil moisture data from a WSNA node tested over one month

As mentioned earlier, the backup battery has a capacity of 200 mAh. Under average current demand of 69.4  $\mu$ A and assuming that the battery is brand new at the time when  $V_C$  goes below 3.6 V, the duration is given by  $200\text{ mAh} / 69.4\mu\text{A}$ , which is approximately 4 months.

We determined that the system is reliable based on the following: 1) The system is able to automatically turn on itself at a desired voltage value; 2) The battery backup voltage decreases at a very slow rate when it is not providing the power supply to the system (i.e., when supercapacitors are supplying power); 3) The system is capable to automatically switch the power source from supercapacitors to battery backup and vice versa at a desired threshold voltage value; 4) The solar panel can charge the supercapacitors quickly; 5) The system can operate under harsh weather conditions; 6) The recorded VWC and soil temperature are accurate within  $\pm 1\%$  and  $\pm 1^\circ\text{C}$ , respectively; and 7) The WSNA successfully recorded and displayed data for six nodes.

Further field tests at various agricultural sites will allow us to determine the long-term impact of the WSNA on irrigation efficiency and operating experience. In addition, these tests will produce data that can be extrapolated to analyze scenarios, in which the proposed system would significantly improve irrigation efficiency.

## V. BENEFITS AND FEASIBILITY

The deployment of a WSNA in large or small farms has an abundance of benefits for both the farmer and the environment alike. A WSNA allows farmers to effectively monitor the health of their cropland to see which locations require irrigation. Consequently, the deployment of a WSNA effectively reduces overwatering, one of the major factors in agricultural water wastage. The WSNA gives invaluable information for farmers to act upon and make crucial decisions that can improve their irrigation efficiency. Furthermore, a WSNA gives farmers the ability to see their farmlands growth over several months and years, and compare it to previous seasons. This gives them a way to explore which methods were more successful. A WSNA will allow farmers to effectively join the modern technological world and increase their agricultural output by using the real-time

information about their crops to stay informed on the growth of their produce.

Compared to solutions available on the market, the WSNA is much more affordable and cost-effective. Comparative industrial wireless sensor nodes cost twice the amount of the WSNA node [20]. Moreover, solutions available on the market do not have other various sensors or even the option for add-on sensors. A base WSNA node not only measures up to six soil moisture probes, but also has the potential to measure various other necessary aspects of a crop's health. Another major feature of the WSNA is its ease of adaptability, as the system can be modified for different circumstances, needs, or preferences of the farmer. Each node can be expanded to add several sensors beyond the basic soil moisture sensor, soil temperature, and pyranometer described here.

Finally, the WSNA has major impacts on the health of the environment through the reduction of overwatering. Wireless soil moisture sensor networks have been shown to greatly improve a farmer's irrigation efficiency, consequently decreasing overall water wastage [21]. This will help reduce the prevalence of droughts and water shortages, which is predicted to affect over two thirds of the world's population by 2025 [22]. The implementation of a WSNA will also give the farmer better information to act upon, so that they can more effectively grow and harvest their crops, increasing food production.

Costs of irrigation water in the US vary greatly with geographic location, water sources, and institutional arrangements. The latter are important because in order to lower food prices, federal and state agencies subsidize irrigation water making its cost much lower than their real cost. As reported a decade ago, the lowest costs are for water from riparian water rights and federal agreements, and vary between \$5 and \$10 per 1,000 m<sup>3</sup> of water (~\$6 and ~\$12 per acre-foot). Intermediate costs, \$20 to \$100 per 1,000 m<sup>3</sup> of water (~\$24 to ~\$120 per acre-foot) correspond to less favorable conditions and arrangements with state agencies. Highest costs exceed \$100 per 1,000 m<sup>3</sup> of water (>\$120/acre-foot) when farmers have to pay market prices [23]. Costs have not varied too much with respect to the 2010 range; e.g., 13-100 \$/acre-foot in Central California [24].

Water consumption varies greatly due to climate conditions, irrigation efficiency, and crop requirements. On average, irrigated farmland in the US consumes ~ 10,000 m<sup>3</sup> of water (~8 acre-foot) per ha per year, varying from ~2,000 m<sup>3</sup> to ~20,000 m<sup>3</sup> of water (~1.6 to ~16 acre-foot) per ha per year [23]. Because of the high variability in costs and consumption of water, we analyze 16 scenarios based on four levels each of unit cost (per 1000m<sup>3</sup>) and annual usage (1000m<sup>3</sup>/ha per year). TABLE 2 illustrates cost in USD per ha per year (obtained by multiplying unit cost and usage). Shaded cells denote scenarios that are not currently realistic, because larger volumes are priced using lower rates (the highest value reported in 2010 was 772 \$/ha [23]). We used scenarios varying between 10 and 750 \$/ha per year for economic evaluation of WSNA deployment.

WSNA's investment value is estimated at 386\$/ha assuming one node per acre (0.404 ha) and 15 nodes per gateway, and that

TABLE 2 IRRIGATION WATER COST PER HA BASED ON UNIT COST AND WATER USE. SHADED CELLS ARE NOT CURRENTLY REALISTIC

Water Cost (\$/ha)		Water unit cost (\$/1000m <sup>3</sup> )			
		5	20	100	150
Water Use (1000m <sup>3</sup> ha <sup>-1</sup> yr <sup>-1</sup> )	2	10	40	200	300
	5	25	100	500	750
	10	50	200	1000	1500
	20	100	400	2000	3000

the cost for one node totals ~152 USD, while one gateway totals ~ 63 USD. We calculate WSNA simple payback period (in years) as WSNA investment (\$386/ha) divided by cost per ha per year under realistic scenarios between 10 and 750 \$/ha shown in TABLE 2, and for a range of 10%-40% increase in irrigation efficiency (TABLE 3). Shaded cells indicate payback periods ranging from slightly larger than 1 year to ~13 years, i.e., shorter than 15 years, and represent the most economically feasible situations for WSNA implementation. As can be noted, favorable economics occur for annual costs exceeding \$50/ha; with payback period decreasing as either annual cost or irrigation efficiency increase.

These results highlight the economic feasibility of implementing WSNA technology in both large and small farmlands. It should be emphasized that these results are based on subsidized irrigation water costs in the USA, and therefore an analysis based on real water costs would yield much shorter payback periods. Moreover, the benefits of installing a resilient irrigation method backed by the WSNA system, especially in semi-arid regions prone to prolonged droughts, is much more than the direct value of saving water. Indeed, the initiative to push for a collective reduction of irrigation water is priceless.

TABLE 3 SIMPLE PAYBACK PERIOD OF WSNA DEPLOYMENT AS A FUNCTION OF IRRIGATION WATER COST AND INCREASE IN IRRIGATION EFFICIENCY. SHADED CELLS INDICATE THE MOST FAVORABLE SITUATIONS

Payback period (yr)		Increase in irrigation efficiency (%)			
		10%	20%	30%	40%
Water Cost (\$/ha)	10	386.0	193.0	128.7	96.5
	25	154.4	77.2	51.5	38.6
	40	96.5	48.3	32.2	24.1
	50	77.2	38.6	25.7	19.3
	100	38.6	19.3	12.9	9.7
	200	19.3	9.7	6.4	4.8
	300	12.9	6.4	4.3	3.2
	500	7.7	3.9	2.6	1.9
	750	5.1	2.6	1.7	1.3

## VI. CONCLUSIONS

In an era where water conservation is dramatically becoming a forefront global issue and water shortages affecting billions of people each year, the WSNA is a comprehensive and cost-effective system that meets the needs of commercial and local farmers while helping solve the major issue of water wastage in farmlands through the reduction of over-watering. We presented the working principles and operating capabilities of the WSNA, analyzed the results of a 4-month long deployment, and discussed the economic benefits. The WSNA was designed through extensive electrical and environmental engineering. If the WSNA technology is implemented in US agriculture, there will be a great increase in overall irrigation efficiency, which will decrease water wastage and positively affect the environment for decades to come. Furthermore, the WSNA technology will increase the economic output of agriculture in the US, through the indirect increase in agricultural productivity as well as the direct savings for each farmer from decreased water consumption. It is imperative for the prosperity of our society that technologies like the WSNA are implemented soon to curb the looming possibility of a global water crisis.

## ACKNOWLEDGMENT

This paper is based on the report and presentation to the 30<sup>th</sup> WERC Environmental Design Contest, Task 2, April 2020, which was awarded the Freeport-McMoRan Innovation in Sustainability Award. We thank the organizers of the contest for the opportunity to participate and the judges of the contest for useful feedback. We are very appreciative of the insightful comments and suggestions from the anonymous reviewers of this paper.

## REFERENCES

- [1] UNESCO, 2019. The United Nations World Water Development Report 2019: Leaving No One Behind.: United Nations Education, Scientific & Cultural Organization. pp.
- [2] Stubbs, M., 2016. Irrigation in U.S. Agriculture: On-Farm Technologies and Best Management Practices. CRS Report. R44158 - Version 7. Washington D.C.: Congressional Research Service. 31 pp.
- [3] Acevedo, M.F., 2011. Interdisciplinary progress in food production, food security and environment research. Environmental Conservation, 38(2):151-171.
- [4] Robinson, D., C. Gardner, J. Evans, J. Cooper, M. Hodnett, and J. Bell, 1998. The dielectric calibration of capacitance probes for soil hydrology using an oscillation frequency response mode. Hydrology and Earth Systems Science, 2.
- [5] Robinson, D.A., C.M.K. Gardner, and J.D. Cooper, 1999. Measurement of relative permittivity in sandy soils using TDR, capacitance and theta probes: comparison, including the effects of bulk soil electrical conductivity. Journal of hydrology, 223(3):198-211.
- [6] Kallioras, A., A. Khan, M. Piepenbrink, H. Pfletschinger, F. Koniger, P. Dietrich, and C. Schuth, 2016. Time-domain reflectometry probing systems for the monitoring of hydrological processes in the unsaturated zone. Hydrogeology Journal, 24(5):1297-1309.
- [7] Kelleners, T.J., M.S. Seyfried, J.M. Blonquist, Jr., J. Bilskie, and D.G. Chandler, 2005. Improved Interpretation of Water Content Reflectometer Measurements in Soils. Soil Science Society of America journal, 69(6):1684-1690.
- [8] Fares, A., F. Abbas, D. Maria, and A. Mair, 2011. Improved Calibration Functions of Three Capacitance Probes for the Measurement of Soil Moisture in Tropical Soils. Sensors, 11(5):4858-4874.

- [9] Kargas, G. and K.X. Soulis, 2012. Performance Analysis and Calibration of a New Low-Cost Capacitance Soil Moisture Sensor. *Journal of Irrigation & Drainage Engineering*, 138(7):632-641.
- [10] Visconti, F., J.M. de Paz, D. Martínez, and M.J. Molina, 2014. Laboratory and field assessment of the capacitance sensors Decagon 10HS and 5TE for estimating the water content of irrigated soils. *Agricultural Water Management*, 132:111-119.
- [11] METER Environment. EC-5 | Soil Moisture Sensor | METER Environment. METER. Accessed April 2020. Available from: <https://www.metergroup.com/environment/products/ec-5-soil-moisture-sensor/>.
- [12] Campbell Scientific. CS655, 12 cm Soil Moisture and Temperature Sensor. Accessed April 2020. Available from: <https://www.campbellsci.com/cs655>.
- [13] Campbell Scientific. HS2 - HydroSense II Handheld Soil Moisture Sensor. 2020/04/06/00:51:34. Accessed April 2020. Available from: <https://www.campbellsci.com/hs2>.
- [14] Acevedo, M.F., 2015. Real-Time Environmental Monitoring: Sensors and Systems. CRC Press. 356 pp. ISBN 978-1-4822-4020-7.
- [15] Zotarelli, L., M.D. Dukes, and M. Paranhos, 2013. Minimum Number of Soil Moisture Sensors for Monitoring and Irrigation Purposes. UF/IFAS Extension HS1222. Gainesville, FL: Horticultural Sciences Department, University of Florida, Institute of Food and Agricultural Sciences (IFAS) 4pp.
- [16] Parris, K., 2010. Sustainable Management of Water Resources in Agriculture. Paris, France: OECD Publishing 118 pp. ISBN 978-92-64-08357-8.
- [17] Digikey. NTCLE100E3 - Vishay BC Components - Thermistors NTC (Negative Temperature Coefficient) | Online Catalog | DigiKey Electronics. 2020/01/08/18:59:30. Accessed April 2020. Available from: <https://www.digikey.com/catalog/en/partgroup/ntcle100e3/10931>.
- [18] Advanced Photonix. Plastic photodiode with leads PDB-C139. 2019. Accessed October 2019. Available from: <https://datasheet.octopart.com/PDB-C139-Advanced-Photonix-datasheet-146011.pdf>.
- [19] Ventura, F., O. Facini, S. Piana, and P. Rossi Pisa, 2010. Soil Moisture Measurements: Comparison of Instrumentation Performances. *Journal of Irrigation & Drainage Engineering*, 136(2):81-89.
- [20] Stoughton, K.M. and R. Butner, 2015. Irrigation Controls Based on Wireless Soil Moisture Technology Assessment: George C. Young Federal Building and U.S. Courthouse, Orlando, FL. April 2020. San Francisco, CA: United States General Services Administration (GSA) Green Proving Ground National Program. 49 pp.
- [21] NCD. Wireless Soil Moisture Sensor Long Range IoT Transmitter. Accessed April 2020. Available from: <https://store.ncd.io/product/wireless-soil-moisture-sensor-greenhouse-iot/>.
- [22] World Economic Forum, 2019. The Global Risks Report 2019, 14th edition Insight Report. Geneva, Switzerland: World Economic Forum. 107 pp. ISBN 978-1-944835-15-6.
- [23] Wichelns, D., 2010. Agricultural Water Pricing. United States. Organization for Economic Co-operation and Development (OECD). 27 pp.
- [24] Central California Irrigation District. Water Supply Update. 2020. Accessed June 2020. Available from: <https://ccidwater.org/wp-content/uploads/2020/05/CCID-Water-Supply-Update-05-28-2020.pdf>.